AD-A232 143

(2)

Unclassified

SECURITY CLASSIFICATION OF THIS PAGE

# REPORT DOCUMENTATION PAGE

Form Approved OMB No. 0704-0188

| | |
|---|---|
| 1a. REPORT SECURITY CLASSIFICATION: Unclassified | 1b. RESTRICTIVE MARKINGS |
| 2a. SECURITY CLASSIFICATION AUTHORITY | 3. DISTRIBUTION/AVAILABILITY OF REPORT: Approved for public release; Distribution unlimited |
| 2b. DECLASSIFICATION/DOWNGRADING SCHEDULE | |
| 4. PERFORMING ORGANIZATION REPORT NUMBER(S): PL-TR-91-2027 | 5. MONITORING ORGANIZATION REPORT NUMBER(S) |
| 6a. NAME OF PERFORMING ORGANIZATION: Phillips Laboratory, Geophysics Directorate; 6b. OFFICE SYMBOL (If applicable): PHP | 7a. NAME OF MONITORING ORGANIZATION |
| 6c. ADDRESS (City, State, and ZIP Code): Hanscom AFB, Massachusetts 01731-5000 | 7b. ADDRESS (City, State, and ZIP Code) |
| 8a. NAME OF FUNDING/SPONSORING ORGANIZATION; 8b. OFFICE SYMBOL (If applicable) | 9. PROCUREMENT INSTRUMENT IDENTIFICATION NUMBER |
| 8c. ADDRESS (City, State, and ZIP Code) | 10. SOURCE OF FUNDING NUMBERS |

| PROGRAM ELEMENT NO | PROJECT NO | TASK NO | WORK UNIT ACCESSION NO |
|---|---|---|---|
| 62101F | 7601 | 22 | 02 |

DTIC ELECTE MAR 12 1991 S G D

11. TITLE (Include Security Classification)
Solar Wind Conditions for a Quiet Magnetosphere

12. PERSONAL AUTHOR(S)
K.J. Kerns, M.S. Gussenhoven

| 13a. TYPE OF REPORT | 13b. TIME COVERED | 14. DATE OF REPORT (Year, Month, Day) | 15. PAGE COUNT |
|---|---|---|---|
| Reprint | FROM ______ TO ______ | 1991 February 11 | 9 |

16. SUPPLEMENTARY NOTATION
Reprinted from Journal of Geophysical Research, Vol. 95, No A12, pages 20,867-20,875 December 1, 1990

| 17. COSATI CODES | | | 18. SUBJECT TERMS (Continue on reverse if necessary and identify by block number) |
|---|---|---|---|
| FIELD | GROUP | SUB-GROUP | Quiet magnetosphere, Baseline magnetosphere, Solar wind, Magnetosphere coupling |

19. ABSTRACT (Continue on reverse if necessary and identify by block number)


The conditions of the solar wind that lead to a quiet magnetosphere are determined under the assumption that the quiet or baseline magnetosphere can be identified by prolonged periods of low values of the *am* index. We analyzed solar wind data from 1978 to 1984 (7 years) during periods in which $am \leq 3$ nT to identify those solar wind parameters that deviate significantly from average values. Parallel studies were also performed for prolonged periods of $Kp = 0, 0+$ and $AE < 35$ nT. We find that for quiet times the solar wind velocity ($V$), the interplanetary magnetic field magnitude ($B$), and the z component of the IMF ($B_z$) show distinctive variations from average values. We independently varied these solar wind parameters and the length of time the conditions must persist to minimize *am*. This was done with the additional requirement that our conditions yield a reasonable number of occurrences (5% of the data set). The resulting baseline conditions are $V \leq 390$ km/s; $180° - \arctan|B_y/B_z| \leq 101°$, when $B_z \leq 0$ (no restriction on $B_z$ positive); $B \leq 6.5$ nT; and persistence of these conditions for at least 5 hours. Minimizing the *am* index does not require a clear upper limit on the value of $B_z$ as might be anticipated from the work of Gussenhoven (1988) and Berthelier (1980). Apparently, this is a result of the requirement that the conditions must occur 5% of the time. When the requirement is lowered to 1% occurrence, an upper limit to $B_z$ emerges.


| | |
|---|---|
| 20. DISTRIBUTION/AVAILABILITY OF ABSTRACT: ☐ UNCLASSIFIED/UNLIMITED ☒ SAME AS RPT ☐ DTIC USERS | 21. ABSTRACT SECURITY CLASSIFICATION: Unclassified |
| 22a. NAME OF RESPONSIBLE INDIVIDUAL: M.S. Gussenhoven | 22b. TELEPHONE (Include Area Code): (617) 377-3212; 22c. OFFICE SYMBOL: PHP |

DD Form 1473, JUN 86 — Previous editions are obsolete.

SECURITY CLASSIFICATION OF THIS PAGE
Unclassified

JOURNAL OF GEOPHYSICAL RESEARCH, VOL. 95, NO. A12, PAGES 20,867–20,875, DECEMBER 1, 1990

# Solar Wind Conditions for a Quiet Magnetosphere

K. J. KERNS AND M. S. GUSSENHOVEN

*Geophysics Laboratory, Hanscom Air Force Base, Massachusetts*

The conditions of the solar wind that lead to a quiet magnetosphere are determined under the assumption that the quiet or baseline magnetosphere can be identified by prolonged periods of low values of the *am* index. We analyzed solar wind data from 1978 to 1984 (7 years) during periods in which $am \leq 3$ nT to identify those solar wind parameters that deviate significantly from average values. Parallel studies were also performed for prolonged periods of $Kp$ = 0, 0+ and $AE < 35$ nT. We find that for quiet times the solar wind velocity ($V$), the interplanetary magnetic field magnitude ($B$), and the $z$ component of the IMF ($B_z$) show distinctive variations from average values. We independently varied these solar wind parameters and the length of time the conditions must persist to minimize *am*. This was done with the additional requirement that our conditions yield a reasonable number of occurrences (5% of the data set). The resulting baseline conditions are $V \leq 390$ km/s; $180° - \arctan |B_y/B_z| \leq 101°$, when $B_z \leq 0$ (no restriction on $B_z$ positive); $B \leq 6.5$ nT; and persistence of these conditions for at least 5 hours. Minimizing the *am* index does not require a clear upper limit on the value of $B_z$ as might be anticipated from the work of Gussenhoven (1988) and Berthelier (1980). Apparently, this is a result of the requirement that the conditions must occur 5% of the time. When the requirement is lowered to 1% occurrence, an upper limit to $B_z$ emerges.

## 1. INTRODUCTION

*Gussenhoven* [1988] suggested that a useful definition of a baseline magnetosphere is a magnetosphere in which coupling with the solar wind is minimized. She reviewed magnetospheric particle, current and electric field data to show that minimum coupling occurs when the solar wind velocity ($V$) and the interplanetary magnetic field (IMF) magnitude ($B$) are small, as at the end of a well-formed solar wind sector. She also found evidence that weaker conditions occur when the IMF north-south component ($B_z$) is near zero, rather than for strongly northward conditions which produce an active polar cap. In addition, a relaxation time is required for the magnetosphere to attain a quiet state. She proposed the following conditions for the baseline magnetosphere: $B < 5$ nT, $|B_z| < 2$ nT, $V < 400$ km/s, and persistence of these conditions for 2–4 hours before the baseline magnetosphere is reached.

There are many statistical studies relating solar wind parameters and magnetospheric activity [see *Baker*, 1986; *Akasofu*, 1981, and references therein]. By far the greatest effort has been to determine the drivers of active, or storm and substorm conditions. These efforts show that magnetospheric magnetic activity is proportional to the magnitude of both $B_z$ (when it is southward) and $V$ [*Arnoldy*, 1971; *Burton*, 1975; *Akasofu*, 1979; *Berthelier*, 1980; *Maezawa and Murayama*, 1986]. Increased $B$ and ion temperature are also associated with increased magnetic activity [*Berthelier*, 1980]. *Wilcox and Ness* [1965] related the periodic nature of geomagnetic storms and substorms to solar wind sector changes, showing that geomagnetic activity is greater at the leading edge of sectors, as is $V$ and $B$. Auroral activity as measured by the auroral electrojet index, $AE$, diminishes when $B_z$ becomes small, or positive [*Hoffman et al.*, 1988]. However, *Berthelier* [1980], *Brautigam et al.* [1988], and *Hardy et al.* [1981] give evidence that magnetospheric activity does not continue to decrease as $B_z$ becomes strongly positive and that activity may actually increase in this range. The objective of this research is to determine the set of solar wind conditions that lead to a quiet magnetosphere when "quiet" is determined by magnetic indices.

We consider three magnetic indices to be appropriate for this study: $Kp$, $AE$, and *am*. The $Kp$ index correlates well with other methods of specifying magnetospheric activity such as the total energy flux of auroral precipitation [*Brautigam et al.*, 1988], the location of the auroral equatorward boundary [*Galperin et al.*, 1977; *Gussenhoven et al.*, 1981], and the magnitude of magnetospheric electric fields [*Kivelson*, 1976]. $Kp$ is a 3-hour index formed from $K$ index data obtained from 12 stations around the world ranging in geomagnetic latitudes from 48° to 63° [*Knecht and Shuman*, 1985]. Its major drawback is that using time averages of $K$ indices to show average activity can be misleading because the $K$ indices are logarithmic in nature. Average activity is better shown by using data measured on linear scales. The $Kp$ index is converted to a linear scale in the *ap* index, but because it is originally defined using $K$ indices from individual stations, *ap* is limited to 28 values ranging from 0 to 400 nT, instead of a smooth distribution of values. The hourly $AE$ index is a monitor of activity in the auroral zones (60°–71°) [*Kamei and Maeda*, 1982]. The hourly values of this index are complete from 1978 to 1984. Because it uses magnetic variations only in the auroral zones, it is not sensitive to magnetospheric compressions or activity caused by northward $B_z$ [*Berthelier*, 1980]. The *am* index [*Menvielle and Berthelier*, 1988] is a 3-hour planetary index which is an improvement on the $Kp$ index. Although *am* has similar coverage in latitude as $Kp$, the longitudinal distribution of geomagnetic stations is better, and a linear scale is maintained throughout the accumulation and averaging process [*Knecht and Schuman*, 1985]. Thus the *am* index gives a smooth distribution of values ranging from 0 to greater than 400 nT. We perform this study using all three indices but report here the details of results using only the *am* index because of its advantages over $Kp$ and $AE$. Results using the $Kp$ and $AE$ indices were very similar to those using the *am* index. The solar wind conditions are specified by hourly



Paper number 90JA01597.



91 2 26 090

National Space Science Data Center (NSSDC) data for 7 years from 1978 to 1984 [*Couzens and King*, 1986]. The data base covers a large enough period of time that seasonal and diurnal effects, discussed by *Berthelier* [1976], will be averaged out.

This report is organized into two parts. In section 2 we identify the solar wind parameters, which when limited, lead to a quiet magnetosphere. In section 3 we determine the best way to limit the solar wind parameters in order to give the lowest magnetospheric activity while, at the same time, maintaining a significant number of occurrences (5% of the data base).

## 2. Identification of Important Driving Parameters

If the solar wind is the driver of major magnetospheric processes whose times scales are of the order of hours, then certain solar wind conditions will lead to a quiet magnetosphere, one exhibiting minimal magnetic activity on the same time scales. These conditions may involve restrictions on some or all of the solar wind parameters. If the magnetosphere has the capability of storing some of the energy transferred from the solar wind, then this storage capability will cause a delay in the magnetosphere's reflection of solar wind conditions. Magnetospheric activity may be high as long as stored energy is dissipated. Likewise, the magnetosphere may remain quiet at the onset of energy transfer from the solar wind to the magnetosphere.

We define as significant solar wind parameters for the quiet magnetosphere those parameters which when restricted for extended periods lead to low values of *am*. We identify these parameters in the first instance by examining prolonged periods of low values of *am* and finding which solar wind parameters are significantly different from the average solar wind values. The identification is aided by also comparing the distributions of values of solar wind parameters during quiet times to those occurring when there are no restrictions on geomagnetic activity.

Several solar wind parameters are considered here. The solar wind plasma parameters are ion bulk flow speed $V$ (in km/s), ion temperature $T$ (in K), and ion number density $N$ (in $cm^{-3}$). The interplanetary magnetic field (IMF) parameters are the magnitude of the IMF, $B$ (in nT) and its three vector components, $B_x$, $B_y$, and $B_z$. The components are given in geocentric solar magnetospheric (GSM) coordinates. We also order magnetic activity by the arctan $|B_x/B_y|$, the magnitude of the component of the IMF normal to $\hat{x}$ ($B_n$), and $\theta$ where $\theta \equiv$ arctan $|B_y/B_z|$ for $B_z > 0$ and $180° -$ arctan $|B_y/B_z|$ for $B_z < 0$. The arctan $|B_x/B_y|$ relates the direction of the $x$ and $y$ components of the IMF with respect to $\hat{x}$. The variable $\theta$ gives information on the direction of the IMF component normal to $\hat{x}$ independent of its magnitude. $B_n$ gives information on the magnitude of $B$ perpendicular to the solar wind velocity, which relates to the convection electric field.

A data base for quiet times is formed that lists every hour in which $am \leqq 3$ nT and is preceded by exactly 6 hours of $am \leqq 3$ nT. Thus quiet periods which are longer than 9 hours are included only once, and zero hour for these periods is the seventh hour of quiet. The *am* index is less than or equal to 3 nT approximately 5% of the time. The data base covers the years 1978–1984. The 6-hour requirement is longer than the expected delay in the magnetosphere's reaction to solar wind conditions thereby giving us confidence that a stable quiet period has been identified. For each of these "quiet" hours the hourly averaged solar wind and IMF parameters are retained and averaged.

TABLE 1. Comparison of the 7-Year (1978–1984) Average Values of Solar Wind Parameters and Magnetic Indices to the Average Quiet Values

| Parameter | Quiet Value | Normal Value | Ratio of Change |
|---|---|---|---|
| *am*, nT | 1.7 ± 0.9 (121) | 25. ± 27. (61368) | 27.0 |
| $V$, km/s | 340 ± 50 (95) | 430 ± 100 (45459) | 1.8 |
| $T$, 1000 K | 34. ± 28. (66) | 81. ± 80. (30793) | 1.7 |
| $N$, $cm^{-3}$ | 7.8 ± 5.2 (95) | 9.3 ± 7.2 (43784) | 0.3 |
| $B$, nT | 5.3 ± 1.6 (94) | 7.4 ± 3.4 (43831) | 1.3 |
| $B_x$, nT | −0.1 ± 3.6 (94) | −0.1 ± 4.4 (43831) | 0.0 |
| $B_y$, nT | −0.3 ± 3.1 (94) | 0.2 ± 4.9 (43831) | 0.0 |
| $B_z$, nT | 1.8 ± 1.8 (94) | 0.0 ± 3.8 (43831) | 1.0 |
| $\theta$, deg | 59. ± 35. (94) | 90. ± 44. (43831) | 0.9 |
| $\|B_x\|$, nT | 3.2 ± 1.7 (94) | 3.7 ± 2.4 (43831) | 0.3 |
| $\|B_y\|$, nT | 2.6 ± 1.8 (94) | 3.9 ± 3.0 (43831) | 0.7 |
| $B_n$, nT | 3.6 ± 1.9 (94) | 5.3 ± 3.3 (43831) | 0.9 |

Seventh hour of $am \leq 3$ nT for 9 hours. Number of data points is shown in parentheses.

Table 1 shows the average values of the solar wind parameters for the complete 7-year period (normal value) and the average values for the selected quiet hours during the 7 years (quiet values). We reiterate that the "quiet value" is the average of the given quantity for the data base created of points of the seventh consecutive hour of $am \leqq 3$ nT. The sample standard deviation for each parameter is also listed. The number of data points for each parameter is shown in parentheses. The column labelled "ratio of change" shows the ratio of the difference between the quiet and normal averages to the quiet sample standard deviation. This ratio is indicative of how significant the change in the average value is with respect to the statistical uncertainty of the data. If the ratio is close to 1 or higher, the change is considered significant.

In conjunction with the average values listed in Table 1, we show in Figures 1*a*–1*e* how the solar wind plasma parameters vary before, during, and after extended quiet periods. The plots are the result of a 42-hour epoch analysis in which hour zero (the shaded region) is the seventh consecutive hour of $am \leqq 3$ nT (i.e., the hour used in the "quiet value" average). For each hour identified in the quiet time data base, the hourly averaged values of a given parameter from 24 hours prior to 17 hours after hour zero are added to an array with corresponding elements ranging from −24 to 17. Since the solar wind data sets are not complete, a second array counts the number of values added to each element in each array. For each point in the array, the average of each parameter is determined. In Figures 1*a*–1*e* these are displayed all in the same format. The dashed line shows the average value of the given parameter over the entire 7-year period for all *am* values (that is, the normal value listed in Table 1); dashed lines were not shown for averages very close to zero.

We now consider the average values and the ratio of change in Table 1 and the temporal variation of parameters around the quiet hour to determine those parameters that best characterize conditions for a quiet magnetosphere. In

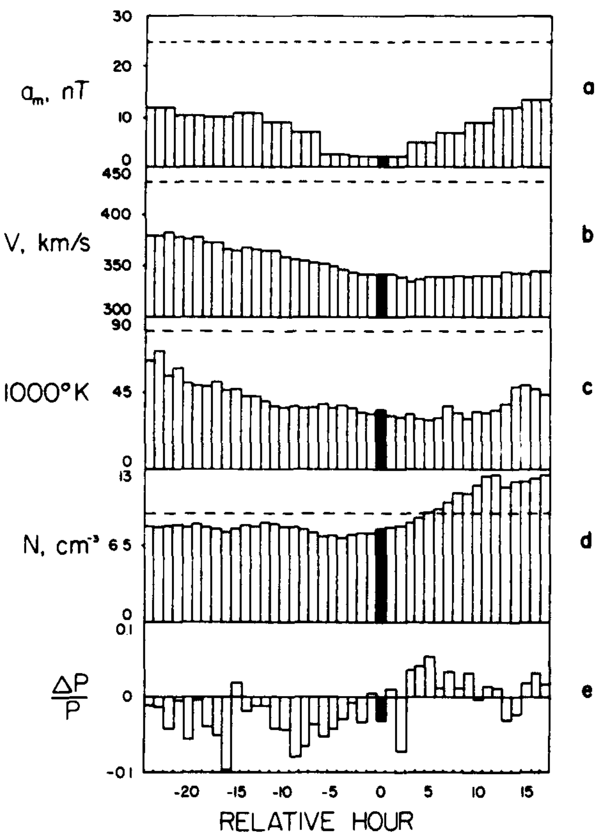


Fig. 1. Time variation of the average values of (*a*) *am* and (*b*) the solar wind velocity, (*c*) temperature, (*d*) density, and (*e*) relative change in dynamic pressure, during periods of extended *am* ≦ 3 nT (hour −6 to hour 2). The dashed lines indicate unrestricted 7-year averages, and no dashed line indicates this average was near zero.

Table 1 and Figure 1*a* the values for *am* are given first for reference. Since restrictions on *am* were used to define the quiet periods, *am*, of all the parameters, has the highest ratio of change. The number of 7-hour periods of *am* ≦ 3 nT is 121. All hours in the epoch analysis have the same number of occurrences since *am* is a complete data set from 1978 to 1984. The values for three consecutive hours are identical, as is expected, because *am* is a 3-hour index. Of particular interest in Figure 1*a* is the fact that 9-hour periods of *am* ≦ 3 nT occur in prolonged periods of magnetic quiet. The overall average value of *am* is 26 nT, but in the near 2-day period surrounding the quiet period, the epoch average *am* remains below 14 nT. Not shown in Figure 1 are the results of the same epoch analysis for *an* and *as* (the northern and southern hemisphere indices of which *am* is the average), *Kp* and *AE*. All indices show the same type of variation that *am* shows, all being severely depressed throughout the whole 42-hour period compared to average values. In particular, for the Kp study the zero-hour average value of *Kp* is 0.3, the maximum reached in the 42 hour epoch is 1.6, while the 7-year average is 2.6. Similarly, for the *AE* study, the zero-hour average value of *AE* is 25 nT, the 42-hour maximum value is 135 nT, while the 7-year average is 245 nT.

Figure 1*b* shows the epoch variation of the solar wind velocity *V*. Note that the range of the *y* axis starts at 300 km/s instead of zero. *V* is significantly depressed during the quiet periods. This is expected since the rate of energy transfer from the solar wind to the magnetosphere, all else being equal, is proportional to *V*. This parameter has the highest ratio of change of any of the solar wind plasma parameters. Figure 1*b* shows that the epoch average values of *V* under quiet restrictions on *am* change only slowly in the 42-hour period, decreasing from 380 to 340 km/s at hour zero and staying essentially constant for the next 17 hours. The 7-year average value with no *am* restrictions is 430 km/s. The solar wind ion temperature *T* is also significantly depressed. Figure 1*c* shows that for at least 24 hours prior to hour zero *T* decreases, and the decrease is by more than 50%. Because *T* is highly variable on relatively short time scales, we found it unreliable as an indicator of quiet.

*N* is not significantly depressed from normal values during the quiet period (Figure 1*d*). The epoch analysis shows, however, that *N* increases to greater than normal values for positive elapsed time, that is, after the extended period of quiet. This is the clearest indication we find that extremely quiet periods may often occur prior to a sector change as suggested by *Gussenhoven* [1988]. *Wilcox and Colburn* [1970] have shown that, on average, sector changes are preceded by increases in *N*, while *V*, ***B***, and magnetic activity remain at minimal levels. To pursue this point further, we examined the 121 quiet periods identified in this analysis for sector changes near hour zero. Only 60 cases have good IMF coverage (90% complete) for the hours from −24 to +25. Of these 60 cases, 48 indicate one or more large-scale changes in the sign of the hourly value of $B_y$ within 24 hours of hour zero. We thus conclude that extended periods of magnetic quiet, as identified here, have high probability of being found prior to sector changes.

The epoch analysis indicates a tendency for the average solar wind dynamic pressure ($\propto NV^2$) to decrease before a quiet period and increase after a quiet period, since the average *V* decreases before and during the quiet period and the average *N* increases afterward. Because a change in dynamic pressure is a mechanism to add or extract energy from the magnetosphere through compressions and expansions, we study the dimensionless parameter $\Delta P/P$ to determine how often additional decreases in dynamic pressure occur within the quiet period. $\Delta P/P$ is defined as $1 - NV^2(h-1)/NV^2(h)$, where *h* indicates the current hour and $h - 1$ indicates the previous hour. Average values of $\Delta P/P$ are determined by calculating individual hourly values of $\Delta P/P$ and then averaging them. Figure 1*e* shows the variation of $\Delta P/P$ for the epoch. We first note that $\Delta P/P$ is negative for many hours preceding and throughout the quiet periods, indicating a trend for the pressure to lessen. The rate of decrease peaks between −5% and −10% per hour. Following the zero hour, $\Delta P/P$ is positive, indicating a state of increasing pressure. This is no doubt related to the sector tendency for *N* to increase as well. After several hours, $\Delta P/P$ is variable, which is the condition we might normally anticipate. The peak average variation of $\Delta P/P$ from zero was −10% (hour −16), whereas the sample standard deviation of that hour was roughly 44%. During hours −9 to −1 where there was a definite trend for $\Delta P/P$ to decrease, the sample standard deviation for each hour was 3–6 times greater than the offset from zero. This indicates there were almost as many increases in $\Delta P/P$ during the quiet periods as decreases. In the period immediately preceding and during the quiet period, the maximum sample standard deviation was 44%, indicating very few occurrences of $\Delta P/P$ of magnitude

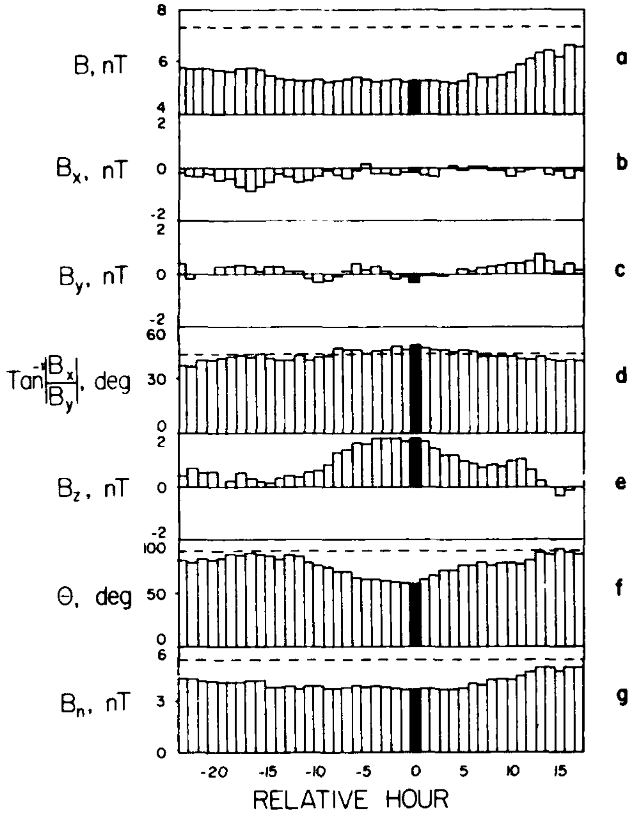


Fig. 2. Time variation of the average values of (*a*) the IMF magnitude, (*b*) *x* component, (*c*) *y* component, (*d*) arctan ($|B_x/B_y|$), (*e*) *z* component, (*f*) $\theta$, and (*g*) the component normal to the velocity, during periods of extended $am \leq 3$ nT (hour −6 to hour 2). The dashed lines indicate unrestricted 7-year averages, and no dashed line indicates this average was near zero.

greater than 50%. A −50% change in $\Delta P/P$ equates to a 1.1 $R_E$ increase in the standoff distance of the dayside magnetopause, a +50% change to a 0.6 $R_E$ decrease in standoff distance. These differences are calculated for a quiet time standoff distance of 9.5 $R_E$ using our average quiet $V$ and $N$ from Table 1. Thus, changes in dynamic pressure that lead to variations in the standoff distance between 8.9 and 10.6 $R_E$ are apparently not large enough to cause the magnetosphere to leave the quiet state as we have defined it.

In Figures 2*a*–2*g* we review the epoch analysis results for the IMF parameters during quiet periods. In Table 1, $B$ shows significant variation from the average during the quiet period. Figure 2*a* shows that $B$ is depressed during the entire period of the epoch analysis compared to the normal value and tends to slowly increase after the end of the quiet period. Note that the range of $B$ in Figure 2*a* is 4–8 nT.

Changes in $B_x$ and $B_y$ are shown in Figures 2*b* and 2*c* and indicate that for prolonged quiet periods there is no directional preference in the *x* or *y* directions of the IMF. The quiet values of $B_x$ and $B_y$ are within ±0.3 nT in the 6-hour period surrounding hour zero. The standard deviations as well as the averages of $B_x$ and $B_y$ were calculated for each hour of the quiet period. We note that the calculated quiet standard deviation of each of these components reaches a minimum during hour zero of the quiet period (not shown). This indicates that the magnitudes of $B_x$ and $B_y$ are limited during the quiet periods. When the magnitudes of $B_x$ and $B_y$ were considered separately, we found that both were somewhat depressed from their average values (see Table 1). Of note is that throughout the period of quiet in the epoch analysis, $|B_x|$ was somewhat greater than $|B_y|$, while before and after the quiet period, $|B_y|$ was dominant. Figure 2*d* shows this trend throughout the epoch using the arctan $|B_x/B_y|$.

The $B_z$ component shifts significantly northward during quiet periods. The mean increases to 1.8 nT from the normal average of 0.0 nT. Figure 2*e* shows that $B_z$ tends to be northward for several hours before the minimum *am*. It returns to normal values much more quickly than does $B$, which is depressed throughout the entire epoch. $\theta$ (Figure 2*f*) also reflects the tendency for the IMF to turn northward during quiet periods. It has a ratio of change and time history similar to that of $B_z$. (Recall that $\theta = 0°$ for $B_z$ strictly northward, 90° for $B_z = 0$, and 180° for $B_z$ strictly southward.)

The epoch analysis indicates that the magnitude of the IMF changes on a much longer time scale than does its direction and that its directional changes include $B_y$ and $B_x$ as well as $B_z$. On average, $B$ is depressed from the 7-year average value up to a day before hour zero of the quiet period. An average $B_z$ begins to have a significant northward component at −8 hours, which is about the same time $\theta$ begins to deviate from the 7-year average value. Similarly, arctan $|B_x/B_y|$ begins its excursion above the average at this time, although this is a much smaller deviation than that of $\theta$. One can deduce from these changes and from the changes in $|B_x|$ and $|B_y|$ (not shown) that the directional changes in the IMF are not only northward but also to greater alignment with the *x* axis. If a greater alignment with the *x* axis contributes significantly to the conditions that create quiet periods, we would expect $B_n = (B_z^2 + B_y^2)^{1/2}$ (which will minimize as $|B_x|$ maximizes) to be more significantly depressed than $B$ during the quiet period. Figure 2*g* shows that $B_n$ moves in the same manner as does $B$, but changes occur more rapidly. $B_n$ is less significantly depressed and has a smaller ratio of change than that of $B$ (Table 1), indicating that directional changes which increase alignment with the *x* axis do not necessarily create quiet conditions.

In summary, the significant parameters for determining prolonged periods of magnetic quiet are identified as the IMF orientation, IMF magnitude, and $V$. Either $\theta$ or $B_z$ can be used to express the orientation of the IMF. By using $\theta$ we avoid repetition of correlation between the magnitude of $B_z$ and magnitude of the IMF. The average values of these quantities are significantly different for extended periods of quiet than for the 7-year average values with no restrictions on magnetic activity. To complete the identification of parameters, we compare the distributions of values of the three parameters for the quiet periods and for no activity restrictions over the 7-year period. Figure 3 gives distributions (in percentage of occurrence) of the three parameters $V$, $B$, and $\theta$ with no restrictions on magnetic activity for 7 years (light shading) and the distributions (in percentage of occurrence) during hour zero of the quiet period (heavy shading). The 7-year distributions have approximately 44,000 data points, and the hour zero distributions have approximately 90 data points. For $B$ and $V$ the quiet distributions are shifted greatly to smaller values, and there is a reasonably clear breakpoint, above which occurrence of high values is small or zero and shows little significance. The breakpoint values are 400 km/s for $V$ and 7 nT for $B$. The distribution of $\theta$ during hour zero is limited to angles less than 90°, while the normal distribution is centered about 90°.

## 3. LIMITING THE PARAMETERS

The parameters $B$, $\theta$, and $V$ are identified in section 1 as important parameters in determining when a quiet magnetosphere occurs. In this section we determine what limits to these parameters cause the resulting average value of *am* to be minimized while allowing a 5% occurrence. In other words, we attempt to specify the range of parameters $V$, $B$, $\theta$ and the time necessary for their persistence in order to guarantee a magnetosphere characterized by low *am*.

Although other studies have investigated the variation of magnetic activity with individual solar wind parameters, we repeat these variations for $V$, $B$, and $\theta$ over the 7 years of our data set. Here we look at the average value of *am* that results if we estrict the range of $V$, $B$, and $\theta$ for four hours. No restrictions are placed on the other two parameters when each of the three parameters are restricted. In every case the value of *am* used is taken in the fourth hour of any period in which the solar wind parameters met the restriction for 4 hours. Averages are performed for the 7 years from 1978 to 1984. Figure 4 shows the results.

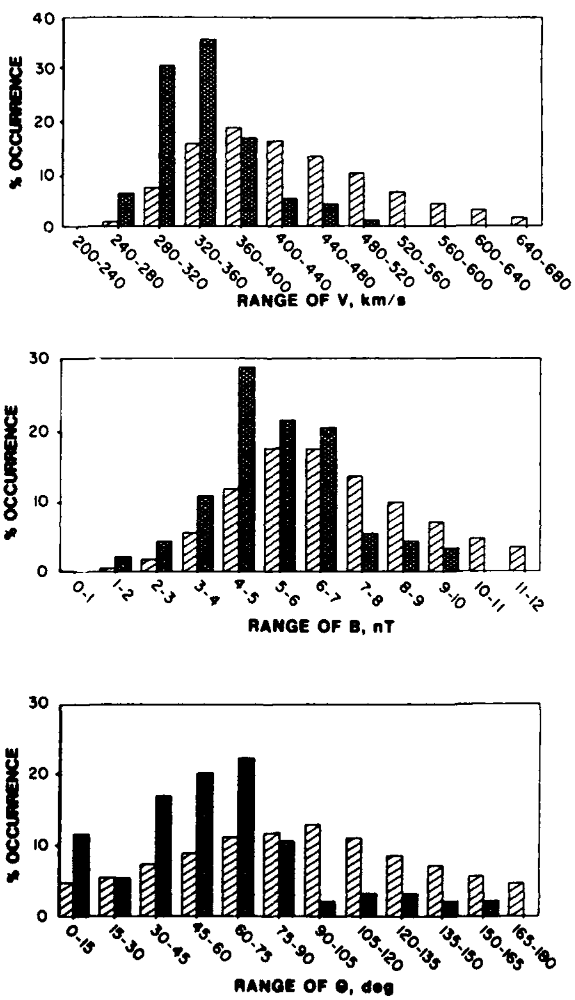


Fig. 3. Normal distribution of solar wind velocity (top), IMF magnitude (middle), and $\theta$ (bottom) for 7-year period of data (light shading) and distribution of those parameters during hour 7 of $am \leq$ 3 nT for 9 hours (dark shading).

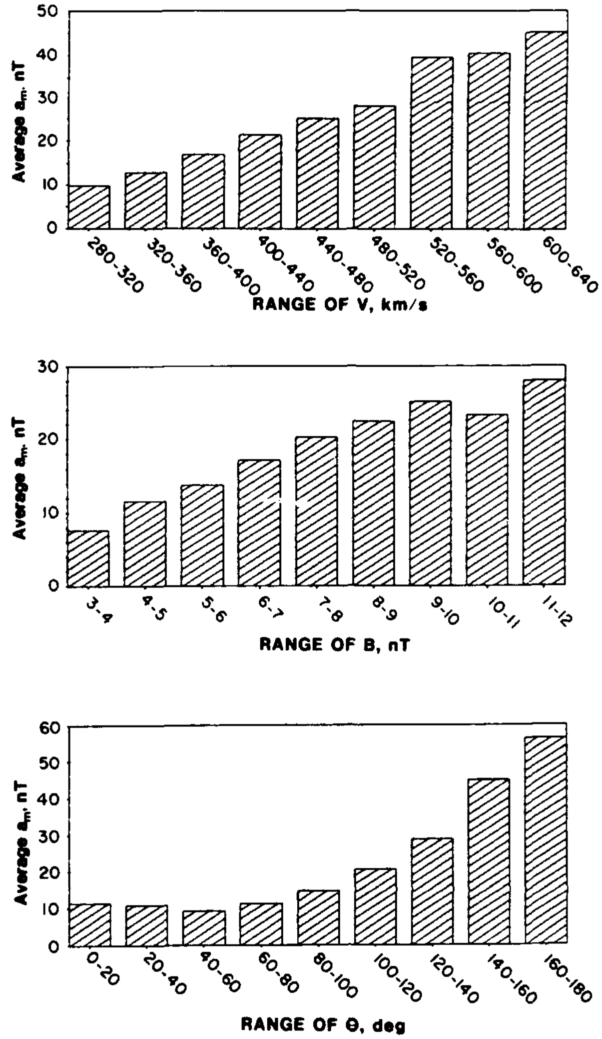


Fig. 4. Average value of *am* when solar wind velocity (top), IMF magnitude (middle), or $\theta$ (bottom) are limited for periods $\geq$ 4 hours.

The average value of *am* varies almost linearly with $B$ and $V$, increasing as the central value of the range of $B$ and $V$ increase. The variations at high $B$ and $V$ are less smooth than the lower values because the number of events in each average is smaller here. The linear increase with $B$ and $V$ indicates that when limiting these two parameters to achieve the lowest *am* value, only upper limits need to be considered. Lower limits are zero, or whatever minimum value the solar wind can achieve. For $\theta$, smaller values (i.e., those with a positive $B_z$ component) generally result in smaller values of *am*. Activity increases sharply as $B_z$ becomes more strictly southward. However, there is some indication that minimum *am* occurs in the range 40°–60° and increases as $B_z$ becomes more northward. This indicates that an upper and lower limit of $\theta$ should be considered when limiting the data.

We attempt to minimize *am*, then, using five variables. These are $B_u$, $V_u$, $\theta_u$, $\theta_l$, and $\Delta t$. The first three variables are upper limits on $B$, $V$, and $\theta$ and the fourth is a lower limit on $\theta$. The final variable $\Delta t$ is persistence and indicates how many hours the first four limits were required to be met. As the limits become more restrictive, the average value of *am* that occurs during periods that meet those limits is expected to decrease. At the same time, more restrictive limits have a lower frequency of occurrence. It is possible to be so restrictive that although the average value of *am* is 0 nT, there are only one or two 1-hour periods in the entire 7-year data set where these cases occur. Since we want our conditions to have meaning, we require limits on the solar wind that are met at least 5% of the time.

The number of occurrences for a given set of limits is a function of the dependent variables $B_u$, $V_u$, $\theta_u$, $\theta_l$, and $\Delta t$. The total number of periods of complete solar wind data sets in the 7-year period of coverage range from approximately 41,300 when $\Delta t$ is 1 hour to 32,000 when $\Delta t$ is 6 hours. Because $\Delta t$ must be an integral number of hours (due to the hourly nature of the data set), it is considered separately from the other limits. The data become less smooth as the number of occurrences decrease due to statistical error, making it difficult to relate the solar wind limits to the number of occurrences. In order to smooth the data relating the number of occurrences as a function of a given set of limits, the data were fit to the general form of the equation

$$y = a_0 + a_1X_1 + a_2X_2 + \cdots + a_nX_n$$

where $y$ is the number of occurrences and $n = 255$. $X_j$ are functions of $B_u$, $V_u$, $\theta_u$, and $\theta_l$ of the form $X_j = B_u^a V_u^b \theta_u^c \theta_l^d$, where $a$, $b$, $c$, and $d$ are integers from 0 to 3 and $j = a + 4b + 16c + 64d$. These ranges were chosen because visual inspection of the data revealed that each limit varied with a significant third- and fourth-order component. Powers greater than three were not used so that high-order variations in the data would be left out and because computing time for the problem increases exponentially. (Note that $a = b = c = d = 0$, results in $X_0 = 1$.) The method of least squares discussed by *Bevington* [1969] results in $n + 1$ simultaneous equations of the form

$$\Sigma y_i = a_0N + a_1\Sigma X_1 + a_2\Sigma X_2 + \cdots + a_n\Sigma X_n$$

$$\Sigma y_iX_j = a_0\Sigma X_j + a_1\Sigma X_1X_j + a_2\Sigma X_2X_j + \cdots + a_n\Sigma X_nX_j$$

The equations were solved by matrix manipulation. A linear correlation between $y$ and the number of occurrences resulted in a correlation of greater than 0.999 for all values of $\Delta t$. Figures 5*a*–5*e* show how the number of occurrences change with each variable. The actual number of occurrences are indicated by the squares, while the crosses indicate the number of occurrences predicted by the fit. Figure 5*a* shows only actual number of occurrences because the fit does not include $\Delta t$ as a variable. Each figure shows how the number of occurrences changes as a single limit is varied over its range, while the other limits are fixed at $\Delta t$ = 4 hours, $B_u$ = 8 nT, $V_u$ = 440 km/s, $\theta_u$ = 90°, and $\theta_l$ = 20°. The ranges of each of the variables shown in Figures 5*a*–5*e* are the ranges for each variable over which the fit was performed. The least squares fit follows the actual data with very little error.

A functional relationship of the same form as that given for the number of occurrences was fit to the average value of *am*. The correlation between measured and fit data was greater than 0.995 for values of $\Delta t$ from 1 to 6 hours. The data set became very rough at $\Delta t$ = 7 hours, resulting in a poor correlation. Figures 6*a*–6*e* show how the average value

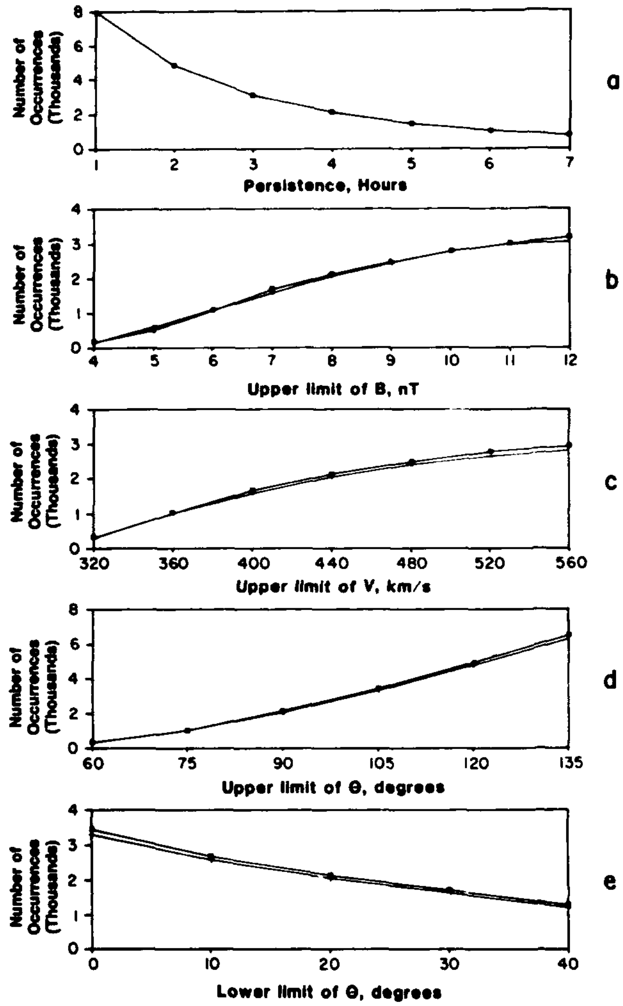


Fig. 5. Number of occurrences in 7 years of the solar wind meeting the solar wind limits $\Delta t$ = 4 hours, $B_u$ = 8 nT, $V_u$ = 440 km/s, $\theta_u$ = 90°, and $\theta_l$ = 20°. These limits were held constant while (*a*) $\Delta t$, (*b*) $B_u$, (*c*) $V_u$, (*d*) $\theta_u$ and (*e*) $\theta_l$ were individually varied. Squares indicate actual numbers of occurrence, while crosses (Figures 5*b*–5*e*) indicate a least squares fit to the number of occurrences.

of *am* changes for the same variables and values given in Figure 5. Quite clearly, more restrictive limits for $\Delta t$, $B_u$, $V_u$, and $\theta_u$ do cause the average value of *am* to decrease.

Activity decreases only slightly as $\theta_l$ increases in Figure 6*e*. Our research has shown that $\theta_l$ has an effect on activity only when $\theta_u$ is small (less than roughly 100°) and when the persistence is greater than 2 hours. The effect of $\theta_l$ increases as $\theta_u$ decreases, and the persistence increases. This is demonstrated in Figure 7 where $\theta_u$ = 60° for the lower curve and 90° for the upper curve and the values of the limits $B_u$, $V_u$, and $\Delta_t$ remain those given for Figures 5 and 6.

The limits to the solar wind parameters which occur 5% of the time and most efficiently lead to a quiet magnetosphere can now be identified. They are identified by minimizing the equation relating average *am* to the solar wind limits with respect to $V_u$, $\theta_u$, and $\theta_l$. $B_u$ is made a function of the other three limits by setting the equation relating the number of occurrences to 5%. At a 5% occurrence, the minimization surface is very smooth and has one minimum in the range of the data. The starting values for the minimizations for each

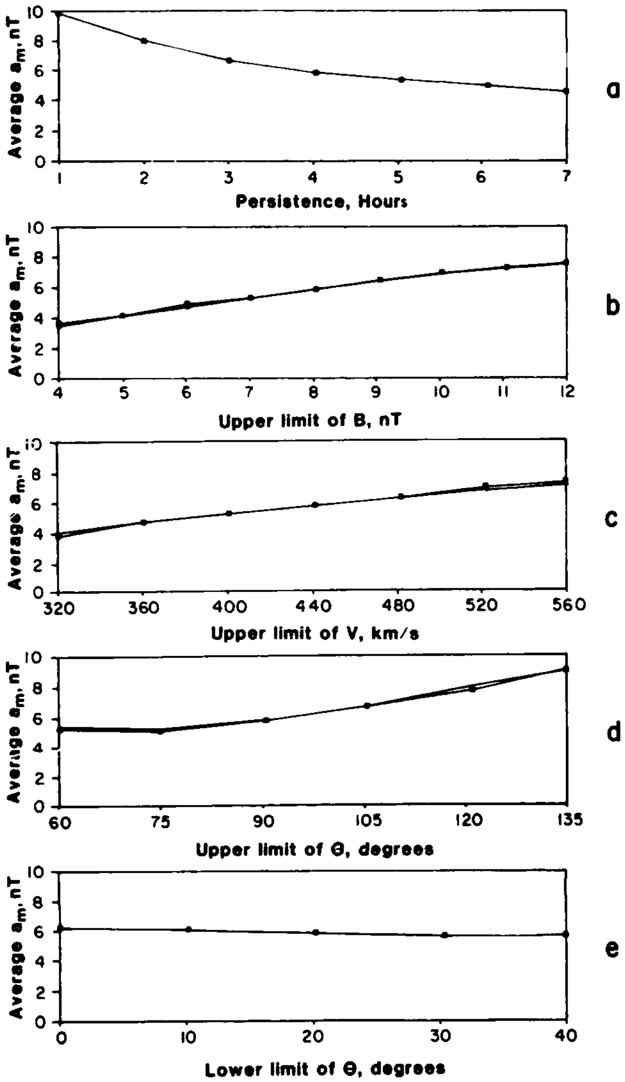


Fig. 6. Average *am* in 7 years of the solar wind meeting the solar wind limits $\Delta t$ = 4 hours, $B_u$ = 8 nT, $V_u$ = 440 km/s, $\theta_u$ = 90°, and $\theta_l$ = 20°. These limits were held constant while (*a*) $\Delta t$, (*b*) $B_u$, (*c*) $V_u$, (*d*) $\theta_u$, and (*e*) $\theta_l$ were individually varied. Squares indicate actual average *am*, while crosses (Figures 6*b*–6*e*) indicate a least squares fit to the average *am*.

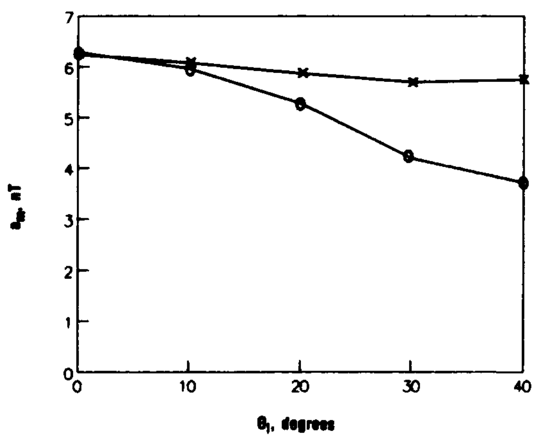


Fig. 7. Variation of the average *am* over 7 years with respect to $\theta_l$. $\Delta t$ = 4 hours, $B_u$ = 8 nT, $V_u$ = 440 km/s, and $\theta_u$ = 90° (upper curve, crosses) and $\theta_u$ = 60° (lower curve, circles).

TABLE 2. Best Set of Limiting Conditions on Solar Wind and Resulting Average *am* at a 5% Occurrence for Different Persistence

| $\Delta t$, hours | $V_u$, km/s | $B_u$, nT | $\theta_u$, deg | $\theta_l$, deg | *am*, nT |
|---|---|---|---|---|---|
| 1 | 340 | 6.0 | 97 | 0 | 6.1 |
| 2 | 350 | 6.2 | 97 | 0 | 5.4 |
| 3 | 370 | 6.3 | 98 | 0 | 5.1 |
| 4 | 380 | 6.4 | 99 | 0 | 5.0 |
| 5 | 390 | 6.5 | 101 | 0 | 4.9 |
| 6 | 400 | 6.7 | 103 | 0 | 5.0 |

value of $\Delta t$ were $V_u$ = 380 km/s, $\theta_u$ = 98°, and $\theta_l$ = 10°. $V_u$, $\theta_u$, and $\theta_l$ were stepped in 1 km/s or 1° increments in the minimization procedure. The solar wind limits identified which most efficiently lead to a quiet magnetosphere for each value of $\Delta t$ are shown in Table 2. The values of $\Delta t$ are in hours, $V_u$ is in kilometers per second and is rounded to the nearest 10, $B_u$ and *am* are in nanoteslas and are rounded off to the nearest tenth, and $\theta_u$ and $\theta_l$ are in degrees and are rounded off to the nearest one.

## 4. RESULTS AND DISCUSSION

The data in Table 2 show a very smooth increase of the solar wind limits as $\Delta t$ changes. As the persistence increases, the other limits become less restrictive as expected. Of the conditions shown in Table 2, those for a persistence of 5 hours give the lowest value of *am*. Figure 8 shows the distribution of *am* that meets the restriction that all solar wind velocity and IMF data is complete for 5 hours (upper curve) and the distribution of *am* that meets the 5 hours limits given in Table 2. The area under the lower curve is roughly 5% the area under the upper curve, and as expected, the distribution of the lower curve of *am* is restricted to very low values.

Although *am* is restricted in the lower curve of Figure 8, there is still a tail on the distribution where relatively high values of *am* occur. The four highest of these values of *am*

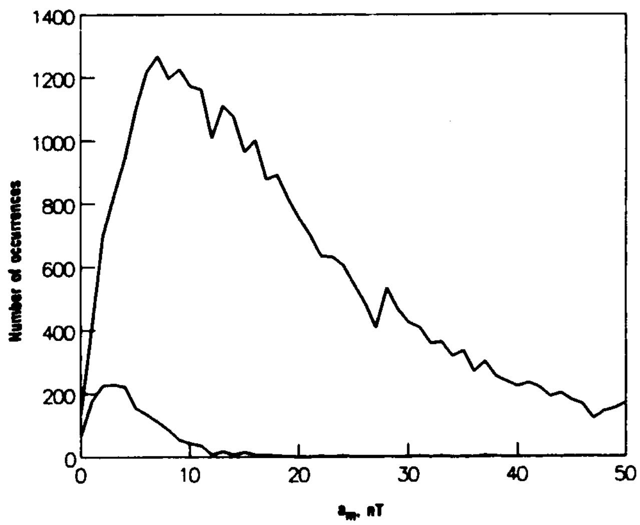


Fig. 8. Number of occurrences of each value of *am* during the 7 years of data during complete 5-hour data sets of IMF and solar wind velocity (upper curve) and during $V \leq 390$ km/s, $B \leq 6.5$ nT, and $\theta \leq 101°$ for at least 5 hours (lower curve).

TABLE 3. Best Set of Limiting Conditions on Solar Wind and Resulting Average *am* at a 1% Occurrence for Different Persistence

| $\Delta t$, hours | $V_u$, km/s | $B_u$, nT | $\theta_u$, deg | $\theta_l$, deg | *am*, nT |
|---|---|---|---|---|---|
| 1 | 320 | 4.7 | 85 | 30 | 4.5 |
| 2 | 320 | 5.4 | 88 | 27 | 3.8 |
| 3 | 330 | 5.7 | 88 | 27 | 3.5 |
| 4 | 350 | 4.9 | 93 | 17 | 3.5 |
| 5 | 380 | 5.0 | 92 | 19 | 3.4 |
| 6 | 390 | 5.1 | 94 | 18 | 3.4 |

are 47, 46, 38, and 37 nT. In the $am = 47$ nT case, the quiet conditions were met in the first hour of the 3-hour period over which the time average of *am* was taken. In the next hour of that same period, $V$ increased from 345 to 397 km/s, $T$ increased from 30,502 to 144,815 K, $N$ increased from 16.4 to 30.3 cm$^{-3}$, and $B$ increased from 3.5 to 10.3 nT. The other three cases were also associated with similar changes in the solar wind parameters which occurred within 3 hours after the time the quiet conditions were met. These four cases demonstrate that a major cause of the tail of the distribution is that the *am* data are averaged over 3 hours, while the solar wind data are averaged over 1 hour. As a result, solar wind conditions which generally lead to low values of *am* can be associated with high values when those solar wind conditions occur within 3 hours of conditions which cause high values of *am*.

On the other hand, we note that the conditions we impose "miss" a significant number of low *am* cases (not necessarily long lasting *am* cases). The cases of $am = 0$ nT which were not included by the lower curve in Figure 8 had at least one parameter out of the limits defined by $B_u$, $V_u$, $\theta_u$, $\theta_l$, and $\Delta t$, while either $V$, $B$, or $\theta$ was limited to very quiet values. These results indicate that a possible improvement of quiet conditions may include a parameter that is a product of two or more solar wind parameters such as $B^n V^m$, or a limit may combine two or more limits so that $V \leqq V_u$ or $B \leqq B_u$ but not necessarily both.

For a 5% occurrence of quiet conditions we find no clear indication of a lower limit to $\theta$ as was suggested by *Gussenhoven* [1988]. Upon examination of the data set we find that the 5% occurrence requirement also required the range of $\theta$ ($\theta_u - \theta_l$) to be roughly 100° in width so that $\theta_u$ is greater than 100°. When $\theta_u$ is in this range, $\theta_l$ has little or no effect on the average value of *am*.

A 1% occurrence requirement (Table 3) does show a nonzero lower limit to $\theta$. For this case the width of the range of $\theta$ is narrower, namely, $\theta_u - \theta_l \simeq 60°$. The resultant lower value of $\theta_u$ causes $\theta_l$ to have a significant effect. This data set has more than a single minimum because the variation of average *am* is less smooth at a 1% occurrence. The lowest minimum, found by starting at the point $V_u = 330$ km/s, $\theta_u = 90°$, and $\theta_l = 25°$, was apparent not only by reasonably low values of *am* but by a fairly smooth transition of the values of the limits as $\Delta t$ increased.

In conclusion, the solar wind conditions which occur 5% of the time and cause minimal magnetospheric activity are $V \leqq 390$ km/s, $B \leqq 6.5$ nT, and $\theta \leqq 101°$ with a persistence of 5 hours. These limits are by no means exact and represent the set of limits which give the lowest average value of *am*. There are many combinations of the solar wind limits which result in only slightly higher average values of *am*. The limits determined in this report that lead to minimal magnetospheric activity are very similar to those predicted by *Gussenhoven* [1988] with the exception that there is no upper limit to $B_z$. An upper limit begins to emerge as the requirement for percentage occurrence is decreased.

*Acknowledgments.* We would like to thank the National Geophysical Data Center for kindly supplying the *am*, *as*, and *an* data and the NSSDC for supplying the solar wind and *Kp* data.

The Editor thanks R. A. Hoffman and J. A. Sauvaud for their assistance in evaluating this paper.

## REFERENCES

Akasofu, S.-I., Interplanetary energy flux associated with magnetospheric substorms, *Planet. Space Sci.*, *27*, 425, 1979.

Akasofu, S.-I., Energy coupling between the solar wind and the magnetosphere, *Space Sci. Rev.*, *28*, 121, 1981.

Arnoldy, R. L., Signature in the interplanetary medium for substorms, *J. Geophys. Res.*, *76*, 5189, 1971.

Baker, D. N., Statistical analyses in the study of solar wind-magnetosphere coupling, in *Solar Wind Magnetosphere Coupling*, edited by Y. Kamide and J. A. Slavin, p. 17, Terra Scientific, Tokyo, 1986.

Berthelier, A., Influence of the polarity of the interplanetary magnetic field on the annual and the diurnal variations of magnetic activity, *J. Geophys. Res.*, *81*, 4546, 1976.

Berthelier, A., Relationships between the solar wind and the polar cap magnetic activity, in *Exploration of the Polar Upper Atmosphere*, edited by C. S. Deehr and J. A. Holtet, p. 245, D. Reidel, Hingham, Mass., 1980.

Bevington, P. R., *Data Reduction and Error Analysis for the Physical Sciences*, p. 164, McGraw-Hill, New York, 1969.

Brautigam, D. H., M. S. Gussenhoven, and D. A. Hardy, The IMF $B_z$ and solar wind speed dependence for precipitating ion hemispheric energy flux, *Adv. Space Res.*, *8*(9), 65, 1988.

Burton, R. K., R. L. McPherron, and C. T. Russell, An empirical relationship between interplanetary conditions and *Dst*, *J. Geophys. Res.*, *80*, 4204, 1975.

Couzens, D. A., and J. H. King, Interplanetary Medium Data Book—Supplement 3A, *Rep. NSSDC/WDC-A-R&S 86-04a*, NASA Goddard Space Flight Cent., Greenbelt, Md. 1986.

Galperin, Y. I., J. Crasnier, Y. V. Lisakov, L. M. Nikolaenko, V. M. Sinitsyn, J.-A. Sauvaud, and V. L. Khalipov, The diffuse auroral zone, 1, A model for the equatorial boundary of the diffuse surge zone of auroral electrons in the evening and midnight sectors, *Cosmic Res.*, Engl. Transl., *15*, 362, 1977.

Gussenhoven, M. S., Low altitude convection, precipitation, and current patterns in the baseline magnetosphere, *Rev. Geophys.*, *26*, 792, 1988.

Gussenhoven, M. S., W. J. Burke, and D. A. Hardy, DMSP/F2 electron observations of equatorward auroral boundaries and their relationship to magnetospheric electric fields, *J. Geophys. Res.*, *86*, 768, 1981.

Hardy, D. A., M. S. Gussenhoven, and E. Holeman, DMSP/F2 electron observations of equatorward auroral boundaries and their relationship to the solar wind velocity and the north-south component of the interplanetary magnetic field, *J. Geophys. Res.*, *86*, 9961, 1981.

Hoffman, R. A., M. Sugiura, N. C. Maynard, R. M. Candey, J. D. Craven, and L. A. Frank, Electrodynamic patterns in the polar region during periods of extreme magnetic quiescence, *J. Geophys. Res.*, *93*, 14,515, 1988.

Kamei, T., and H. Maeda, Auroral electrojet indices (AE) for January–June 1979, in *World Data Center C2 for Geomagnetism: Data Book no. 5*, p. 1, Faculty of Science, Kyoto University, Kyoto, Japan, 1982.

Kivelson, M. G., Magnetosphere electric fields and their variation with geomagnetic activity, *Rev. Geophys.*, *14*, 189, 1976.

Knecht, D. J., and B. M. Shuman, The geomagnetic field, in *Handbook of Geophysics and the Space Environment*, edited by A. S. Jursa, p. 4-1, Geophysics Laboratory, Air Force System Command, Hanscom AFB, Mass., 1985.

Maezawa, K., and T. Murayama, Solar wind velocity effects on the auroral zone magnetic disturbances, in *Solar Wind Magnetosphere Coupling*, edited by Y. Kamide and J. A. Slavin, p. 59, Terra Scientific, Tokyo, 1986.

Menvielle, M., and A. Berthelier, In cooperation with M. Siebert, M. Suguira and J. Cardus, Geomagnetic data, 1983, *IAGA Bull. 32, Ser. 32M*, Int. Serv. of Geomagn. Indices, Paris, 1988.

Wilcox, J. M., and D. S. Colburn, Interplanetary sector structure near the maximum of the sunspot cycle, *J. Geophys. Res.*, *75*, 6366, 1970.

Wilcox, J. M., and N. F. Ness, Quasi-stationary corotating structure in the interplanetary medium, *J. Geophys. Res.*, *70*, 5793, 1965.

M. Gussenhoven and K. Kerns, AFGL/PHP, Hanscom AFB, MA 01731.

(Received February 19, 1990;
revised May 23, 1990;
accepted June 12, 1990.)